Toxicology and Applied Pharmacology 288 (2015) 387–398

Contents lists available at ScienceDirect

Toxicology and Applied Pharmacology

journal homepage: www.elsevier.com/locate/ytaap

Resveratrol *via* sirtuin-1 downregulates RE1-silencing transcription factor (REST) expression preventing PCB-95-induced neuronal cell death

Natascia Guida [a,1], Giusy Laudati [b,1], Serenella Anzilotti [a], Agnese Secondo [b], Paolo Montuori [c], Gianfranco Di Renzo [b], Lorella M.T. Canzoniero [b,d], Luigi Formisano [b,d,*]

[a] IRCSS SDN, Naples 80131, Italy
[b] Division of Pharmacology, Department of Neuroscience, Reproductive and Dentistry Sciences, School of Medicine, "Federico II" University of Naples, Via Pansini, 5, 80131 Naples, Italy
[c] Department of Public Health, 'Federico II' University of Naples, Naples, Italy
[d] Division of Pharmacology, Department of Science and Technology, University of Sannio, Via Port'Arsa 11, 82100 Benevento, Italy

ARTICLE INFO

Article history:
Received 16 June 2015
Revised 12 August 2015
Accepted 14 August 2015
Available online 22 August 2015

Keywords:
SIRT1
REST
c-Jun
Resveratrol
PCB-95

ABSTRACT

Resveratrol (3,5,4′-trihydroxystilbene) (RSV), a polyphenol widely present in plants, exerts a neuroprotective function in several neurological conditions; it is an activator of class III histone deacetylase sirtuin1 (SIRT1), a crucial regulator in the pathophysiology of neurodegenerative diseases. By contrast, the RE1-silencing transcription factor (REST) is involved in the neurotoxic effects following exposure to polychlorinated biphenyl (PCB) mixture A1254. The present study investigated the effects of RSV-induced activation of SIRT1 on REST expression in SH-SY5Y cells. Further, we investigated the possible relationship between the non-dioxin-like (NDL) PCB-95 and REST through SIRT1 to regulate neuronal death in rat cortical neurons. Our results revealed that RSV significantly decreased REST gene and protein levels in a dose- and time-dependent manner. Interestingly, overexpression of SIRT1 reduced REST expression, whereas EX-527, an inhibitor of SIRT1, increased REST expression and blocked RSV-induced REST downregulation. These results suggest that RSV downregulates REST through SIRT1. In addition, RSV enhanced activator protein 1 (AP-1) transcription factor c-Jun expression and its binding to the REST promoter gene. Indeed, c-Jun knockdown reverted RSV-induced REST downregulation. Intriguingly, in SH-SY5Y cells and rat cortical neurons the NDL PCB-95 induced necrotic cell death in a concentration-dependent manner by increasing REST mRNA and protein expression. In addition, SIRT1 knockdown blocked RSV-induced neuroprotection in rat cortical neurons treated with PCB-95. Collectively, these results indicate that RSV *via* SIRT1 activates c-Jun, thereby reducing REST expression in SH-SY5Y cells under physiological conditions and blocks PCB-95-induced neuronal cell death by activating the same SIRT1/c-Jun/REST pathway.

Introduction

Polychlorinated biphenyls (PCBs) are a large family of human developmental neurotoxicants comprising 209 possible congeners (McFarland and Clarke, 1989). They are generally divided into two groups: PCB dioxin-like compounds and PCB non-dioxin-like compounds (NDL). The former compounds bind to the aryl hydrocarbon receptor (AhR), thereby exerting a marked toxicity similar to that of polychlorinated dioxins and furans (Weintraub and Birnbaum, 2008). The latter compounds, instead, despite showing a very low affinity for AhR, also induce neurotoxic effects *in vitro* and *in vivo* (Giesy and Kannan, 1998). We have previously shown that the PCB mixture A1254 increases the repressor element 1 (RE1)-silencing transcription factor (REST) mRNA and protein expression (Formisano et al., 2011) through ERK2/Sp1/Sp3 pathway (Formisano et al., 2015a), which, in turn, by recruiting HDAC3 on the Synapsin-1 promoter causes neuronal death in cortical neurons (Formisano et al., 2015b). In mature neurons, REST is quiescent, but it can be reactivated during normal postnatal development, driving the switch from immature to mature NMDA receptors (Rodenas-Ruano et al., 2012). Accordingly, REST has been closely investigated in brain ischemia where it plays an important role in determining neuronal death in hippocampal and cortical neurons (Formisano et al., 2007, 2013, 2015c; Noh et al., 2012). One study, for instance, reports that in insulted hippocampal neurons, casein kinase 1 suppresses activation of REST protein expression, thereby promoting neuroprotection (Kaneko et al., 2014). Recently, there has been a growing interest in resveratrol (RSV) (3,5,4′-trihydroxystilbene), a polyphenol contained in red wine and known to exhibit beneficial effects in

Abbreviations: AP-1, activator protein 1; PCB-NDL, polychlorinated biphenyl non-dioxin-like; RSV, resveratrol (3,5,4′-trihydroxy-trans-stilbene); EX-527, 6-chloro-2,3,4,9-tetrahydro-1H-carbazole-1-carboxamide; SIRT1, sirtuin 1; MS, oligodeoxynucleotide missense; AS, oligodeoxynucleotide antisense; ChIP, chromatin immunoprecipitation; LDH, lactate dehydrogenase; REST, repressor element-1 silencing transcription factor; DCFH-DA, 2′,7′-dichlorodihydrofluorescein diacetate.

* Corresponding author at: Division of Pharmacology, Department of Science and Technology, University of Sannio, *Via* Port'Arsa 11, 82100 Benevento, Italy.
E-mail address: cformisa@unisannio.it (L. Formisano).

[1] Equal contribution: Natascia Guida, Giusy Laudati.

http://dx.doi.org/10.1016/j.taap.2015.08.010
0041-008X/

several neurological disorders such as Alzheimer Disease (Li et al., 2012), Parkinson Disease (Wu et al., 2011), stroke (Morris et al., 2011) and Amyotrophic Lateral Sclerosis (Mancuso et al., 2014). The most commonly cited mechanism of action of RSV is the activation of the longevity factor silent mating type information regulation 2 homolog 1 (SIRT1) protein (Tang, 2010), a histone deacetylase (HDAC) that is basally expressed in the adult mammalian brain, predominantly in neurons (Donmez, 2012). SIRT1 utilizes nicotinamide (NAD^+) (Donmez and Outeiro, 2013) as a substrate to catalyze deacetylation of various substrates involved in a broad range of physiological functions, including control of gene expression, metabolism, and aging (Rahman and Islam, 2011). Considering the role played by REST in PCB-induced neurotoxicity, here we explored the mechanism by which resveratrol-induced activation of SIRT1 blocks neurotoxicity after PCB exposure. For this study, we evaluated how RSV *via* SIRT1 regulates REST mRNA and protein expression in human neuroblastoma SH-SY5Y cells. Furthermore, we studied the effect of NDL PCB-95 alone or in combination with RSV on the survival of cortical neurons and its correlation with REST.

Material and methods

Drug and chemicals

The compound 2,3,6-2′,5′-pentachlorinated biphenyl (PCB-95) (cod: RPC-130AS) (stock solution 305 μM) was purchased from Ultra Scientific (North Kingstown, RI, USA). Culture media and sera were obtained from Invitrogen (Milan, Italy). The SIRT1 activator 3,5,4′-trihydroxy-trans-stilbene resveratrol (RSV) (cod. R5010; stock solution 10 mM), H_20_2 (cod. H1009; stock solution 10 mM) and the 2′,7′-dichlorofluorescin diacetate (DCFH-DA) (cod: D6883) were obtained from Sigma-Aldrich (St. Louis, MO, USA). The SIRT1 inhibitor 6-chloro-2,3,4,9-tetrahydro-1H-carbazole-1-carboxamide EX-527 (cod. sc-203044; stock solution 20 mM) was obtained from Santa Cruz Biotechnology (Santa Cruz, CA, USA). For those requiring dilution in DMSO, the final DMSO concentration was 0.1% (vehicle). Under these conditions, DMSO did not induce cellular toxicity.

Cell lines and culture conditions

Human neuroblastoma SH-SY5Y cells between the 10th and 30th passage (IRCCS Azienda Ospedaliera Universitaria San Martino-IST-Istituto Nazionale per la Ricerca sul Cancro, Genoa, Italy) were grown as previously published (Cocco et al., 2015). Cells were incubated for 24 h with RSV and EX-527 at 1, 2, 5, and 10 μM and with PCB-95 at 1, 2, 4, 8 and 16 μM. For time-dependent experiments, cells were treated with 8 μM RSV and 5 μM EX-527 for 6, 12, 24, and 36 h. Furthermore RSV and EX-527 (both at 5 μM for 24 h) were simultaneously added to the medium to study the effect on REST and c-Jun mRNA and protein expression and the binding of c-Jun, RNA Pol II, and histone H4 acetylation on REST gene promoter. To evaluate the effects of PCB-95-induced cell toxicity, SH-SY5Y cells were seeded and treated for 24 h with PCB-95 at 1, 2, 4, 8, and 16 μM. Then, the effects of RSV on PCB-95-induced neurotoxicity were explored by seeding and treating cells for 24 h with RSV at 0.25, 0.5, 0.1, 1, 5 and 10 μM, alone or in combination with 8 μM PCB-95. All the above mentioned experiments were performed in DMEM medium containing 1% FBS to avoid loss of the PCB-95 effect through binding to serum component. The experiments on cortical neurons (DIV7) were approved by the Animal Care Committee of "Federico II", University of Naples, Italy and prepared as previously described (Formisano et al., 2015b). In brief, cells were treated for 24 h with PCB-95 at 1,2,4, 8, and 16 μM, and with RSV at 6.25, 12.5, and 25 μM. To study the effects of RSV on PCB-95-induced neurotoxicity, neurons were seeded and treated for 24 h with vehicle, or with RSV 25 μM alone or in combination with 8 μM PCB-95. All these experiments were performed in serum-free neurobasal medium. SH-SY5Y cells were plated in 24-multiwell plates at a density of 2×10^4 for the LDH assay, in 6-multiwell plates at a density of 2.5×10^6 for the determination of free radical production and in 100-mm well plates at a density of 10×10^6 for qRT-PCR, Western Blot, and ChIP analyses. Cortical neurons were plated in 24-well plates at a density of 1×10^6 for LDH, and in 100-mm well plates at a density of 15×10^5 for qRT-PCR and Western Blot analyses.

Cell transfection

Anti-sense (AS) and missense (MS) phosphorothioate oligonucleotides (ODNs) against human SIRT1, p65 (AS SIRT1, AS p65, MS SIRT1, and MS p65), and human and rat c-Jun (AS c-Jun and MS c-Jun) were transfected into SH-SY5Y cells and cortical neurons at a concentration of 1 μM (Guida et al., 2014). Afterward, Opti-MEM was removed and cells were incubated in fresh medium for 24 h. Western blot was subsequently carried out to test the knockdown efficiency. After ODN transfection, experiments with PCB-95 alone or in combination with RSV were carried out. In brief, cells were incubated for 24 h with 8 μM PCB-95 alone or in combination with 5 μM RSV in SH-SY5Y cells or with 25 μM RSV in cortical neurons. MS and AS oligonucleotides against human SIRT1, c-Jun, p65 mRNA, and rat c-Jun mRNA have already been published (Ohkawa et al., 1999; Peterson et al., 2002; Hsieh et al., 2008; Busch et al., 2012). SIRT1 silencing in cortical neurons by small interfering RNA (siRNA) was carried out as previously reported (Formisano et al., 2015b). In brief, cells were transfected with scrambled control (siCTL; sc-37007) and siRNAs against rat SIRT1 (siSIRT1; sc-108043) at 400 nM (Santa Cruz Biotechnology, Santa Cruz, CA).

After siRNA transfection, cells were incubated in a fresh medium for 24 h. Next, they were collected and subjected to western blotting to assess knockdown efficiency. Alternatively, neurons were exposed to PCB-95 (8 μM) alone or in combination with RSV (25 μM) for 24 h. For SIRT1 overexpression experiments in SH-SY5Y cells, cells were transfected with the empty vector pECE; the plasmid carrying SIRT1 cDNA was purchased from Addgene (cod: 1791) (Brunet et al., 2004).

For Western Blot and qRT-PCR analyses, cells were plated in 100-mm dishes and transiently transfected for six hours with 15 μg of DNA using Lipofectamine suspended in Opti-MEM. Next, Opti-MEM was removed and replaced with fresh medium and cells were left to incubate for 24 h. To evaluate cell transfection efficiency, siRNAs and ODNs were mixed with a plasmid encoding the enhanced green fluorescent protein marker; a florescence density of 50% for SH-SY5Y cells and 30%–50% for cortical neurons, respectively, was detected (data not shown).

Lactate dehydrogenase (LDH) assay

LDH Cytotoxicity Kit (1000882) (Cayman, DBA, Milan, IT) was used to assess cell death. LDH efflux into the medium was measured after cortical neurons and SH-SY5Y cells were exposed to PCB-95 alone or in combination with RSV for 24 h, respectively (Formisano et al., 2015b). Triton X-100 Sigma-Aldrich (St. Louis, MO, USA) was used as a positive control for cytotoxicity and its value was considered 100%.

Determination of reactive oxygen species (ROS) production

SH-SY5Y cells were treated with PCB 95 (8 μM) and RSV (5 μM), alone or in combination, for 6 h and H_2O_2 (600 μM) for 30 min. After that ROS production was measured by 2′,7′-dichlorodihydrofluorescein diacetate (DCF-DA) (Molecular Probes, Irvine, CA, USA) as previously described (Amoroso et al., 1999; Pannaccione et al., 2005). Specifically, cells were loaded with 10 μM DCF-DA for 30 min at 37 °C, in a medium whose composition was in mM: NaCl 138, KCl 2.7, $CaCl_2$ 1.2, $MgCl_2$ 1.2, PBS 10, glucose 10, pH 7.4 (standard medium). After the loading period, cells were washed thrice and the reaction was stopped by addition of 2,6-di-tert-butyl-4-methylphenol (0.2% in ethanol) and EDTA (2 mM). Images were acquired by a fluorescence microscope (Nikon Eclipse

E400) using an excitation wavelength of 488 nm. Then, images were analyzed by ImageJ software.

Western blot analysis

Western blot analysis was performed as described elsewhere (Formisano et al., 2011, 2015a; Sirabella et al., 2012; Guida et al., 2014). Cells were lysed in lysis buffer containing 50 mM Tris–HCl, pH 7.4, 150 mM NaCl, 1 mM EDTA, 1% Triton X-100, and protease and phosphatase inhibitors. Samples (100 μg REST, SIRT1, Sp1, Sp3 and 70 μg c-Jun, phospho-c-Jun (p-c-Jun), p65, phospho-p65 (p-p65), calpain, and pro- 3) were subjected to SDS-polyacrylamide gel electrophoresis (SDS-PAGE) and immunoblotted with specific antibodies. Polyclonal antibodies were used against calpain (Formisano et al., 2015b), p-c-Jun (Ser73) (cat: 9164 Cell-Signaling, EuroClone, Milan, IT), c-Jun (cat: sc-1694), p65 (cat: sc-109), p-p65 Ser 536 (cat: sc-33020), p65 (cat: sc-372), SIRT1 (cat: sc-15404), (Santa Cruz Biotechnology, Santa Cruz, CA, USA), and REST (Iannotti et al., 2013; Formisano et al., 2015b); β-Actin (Formisano et al., 2015b) was used as loading control. All antibodies were used at a dilution of 1:1000 except for p-p65 and p-c-Jun (1:250) and β-Actin (1:3000).

Chromatin immunoprecipitation (ChIP) assay

ChIP was performed as previously described (Formisano et al., 2015b). In brief, after 24 h of seeding, cells were exposed to RSV (5 μM) alone or in combination with EX-527 (5 μM) for 24 h. Afterward, cells were cross-linked in 1% formaldehyde for 20 min at room temperature. Cross-linking was stopped by adding glycine at 0.125 M and cells were washed twice in cold PBS containing proteinase inhibitors P-8340 (Sigma-Aldrich St. Louis, MO, USA). Next, they were lysed in 50 mm Tris–HCl buffer (pH 8.1) containing 1% SDS, 10 mm EDTA, and protease inhibitors prepared and sonicated to afford chromosomal DNA in the range of 200–600 bp. At this point, samples were diluted with ChIP dilution buffer (16.7 mm Tris–HCl, pH 8.1, 0.01% SDS, 1.1% Triton X-100, 1.2 mm EDTA, 167 mm NaCl) to a final volume of 1.0 ml. and incubated with protease inhibitors. Twenty microliters of the pre-immunoprecipitated lysate was saved as "input" for later normalization. DNA fragments were enriched by immunoprecipitation with 3 μl anti-P-c-Jun (Ser73) (cat: 9164 Cell-Signaling, EuroClone, Milan, IT), 5 μl anti-H4 acetyl (06-866; polyclonal rabbit antibody; Millipore, Milan, Italy), and 5 μl RNA POL II (R1530; Sigma-Aldrich St. Louis, MO, USA). IgG rabbit antibody was used as a negative control. After thermal cross-link reversion and subsequent proteinase K digestion, DNA was purified by phenol/chloroform extraction followed by ethanol precipitation. The oligonucleotides used for the amplification of the immunoprecipitated DNA of human REST promoter were the following: Fw ChIP A1 5′-CCTGCTACCTGCCACGTCTAGG-3′ Rv ChIP A1 5′-CCGCAGGCTTTGACGG GTC-3, Fw ChIP A2 5′-GCATGCACGCCAGGGCTGGGGGG-3′ Rv ChIP A2 5′-GCCACCGCCCGCGGGACACGCC-3′, Fw ChIP B1 5′-GTGGGGCGCTGG GCTGGGGGC-3′ Rv ChIP B1 5′-C CTCGGTGGAGCGTCCGGGCC-3′, Fw ChIP B2 5′-CCAAGGAGCGGAGCTGCTCGGG-3′ Rv ChIP B2 5′-CACCCC CGCGCCCCGGAAGTTTGCG-3′ Fw ChIP C 5′-GTAACTTTCCGTCCTCTCCC-3′ Rv ChIP C 5′-GGCATTCGGCCATTTTCTC-3′ Fw AP-1 (a) site 5′-CCCG GGCGGCGGCAGTGGC-3′ Rv AP-1 (b) site 5′-CGAGCAGCTCCGCTCCTT GG-3′. The primers used for ChIP on human EPO promoter have already been published (Dioum et al., 2009). The same set of primers used for the B1 site was used for AP-1 (b). PCR was performed with the SYBR Green detection and the results were visualized with ABI PRISM 7000 software (Applied Biosystems) The data were calculated with the $2^{-\Delta\Delta Ct}$ method (Formisano et al., 2015b).

Reverse transcription-real time PCR

Real-time RT-PCR was carried out with cDNAs reverse-transcribed from total RNA by using Light Cycler-FastStart DNA Master SYBR Green I (Roche; 03003230001 Foster City, CA) and ABI PRISM 7000 software (Applied Biosystems) (Formisano et al., 2015b). The primer pairs used for Synapsin-1, NCX1, and β-Actin were the same as those reported elsewhere (Formisano et al., 2011; Vinciguerra et al., 2014). All reactions were performed in triplicate in one assay with a non-template blank for each primer pair as a control for contamination or primer–dimer formation; the cycle threshold (CT) value for each experimental group was determined. The results were normalized to the CT values using the 2-ΔCt formula β-actin in the same sample. Differences in mRNA content between groups were expressed as $2^{-\Delta\Delta ct}$ (Formisano et al., 2015b).

Statistical analysis

Data are expressed as mean ± SEM. Statistical comparisons between the experimental groups were performed using one way ANOVA followed by Newman Keuls test. P value <0.05 was considered statistically significant.

Results

RSV reduces REST mRNA and protein expression in a time- and dose-dependent way in SH-SY5Y cells

SH-SY5Y cells were incubated with a non toxic concentration of RSV (5 μM) (Lee et al., 2007) at different time points (6 to 36 h), and expression levels of REST mRNA were determined by q-RT-PCR. REST mRNA expression was significantly reduced by RSV at 6 h as compared to vehicle, reaching a maximum reduction at 24 h of incubation (Fig. 1a). At 24 h, different concentrations of RSV reduced REST mRNA in a dose-dependent manner (Fig. 1b). Western blot analysis showed that after 12 h of RSV incubation, REST protein expression was significantly reduced, reaching a maximum reduction at 24 h as compared to vehicle (Fig. 1c) in SH-SY5Y cells. In addition, RSV-induced-REST reduction was dose dependent (Fig. 1d). These experiments identified 5 μM of RSV as the concentration that produced an intermediate degree of reduction of REST gene and gene product.

SIRT1 reduces REST mRNA and protein expression in SH-SY5Y cells

It is known that RSV regulates SIRT1 protein expression and deacetylase activity (Seo et al., 2012). q-RT-PCR and Western Blot analysis showed that RSV (5 μM/24 h) did not modify SIRT 1 mRNA and protein expression (Suppl. Fig. 1a and b). Interestingly, when SH-SY5Y cells were treated with the SIRT1 inhibitor EX-527 (1 to 10 μM), REST gene expression and protein levels significantly increased in a dose and time-dependent manner compared with vehicle (Fig. 2a–d). These results suggest that RSV modulates SIRT1 activity, but it has any effects on SIRT1 mRNA and protein. Likewise, when SH-SY5Y cells were treated with RSV in the presence of EX-527, RSV-induced reduction of REST mRNA and protein expression was completely blocked (Fig. 2e,f). To further confirm that RSV through SIRT1 decreases REST protein expression, RSV-treated cells were transfected with specific antisense and missense oligonucleotides for SIRT1 (AS SIRT1 and MS SIRT1, respectively). Notably, AS SIRT1 transfection was able to decrease SIRT1 protein by almost 75% (Suppl. Fig. 2a). As well, AS SIRT1 significantly blocked REST mRNA and protein reduction as compared to cells transfected with MS SIRT1. Interestingly, when cells were transfected with AS SIRT1, REST mRNA and protein expression levels increased (Fig. 2l, m), whereas when they were treated with a construct overexpressing SIRT1 (Brunet et al., 2004) by almost 60% (Suppl Fig. 2b), REST mRNA and protein levels decreased (Fig. 2l, n). We then asked whether REST reduction is functional. To answer this question, we performed q-RT-PCR to examine the gene expression of two REST target genes, *viz*, the sodium\calcium exchanger 1 (NCX1) (Formisano et al., 2013) and Synapsin-1 (Formisano et al., 2011) in SIRT1 silenced or overexpressing

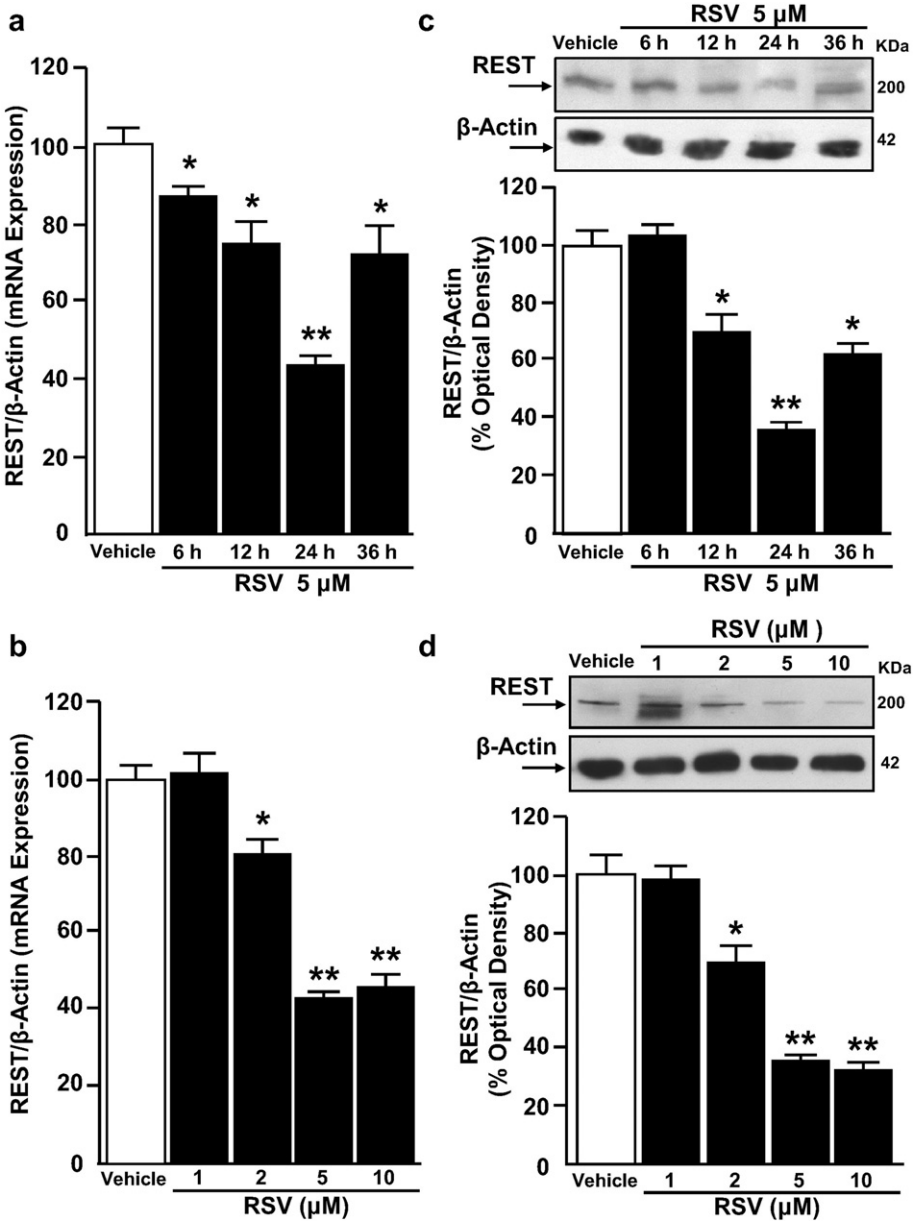

Fig. 1. RSV reduced REST mRNA and protein expression in dose and time dependent manner in SH-SY5Y cells. a,b) q RT-PCR and representative Western blot of REST protein at 6, 12, 24 and 36 h of RSV (5 μM) exposure. Bars represent mean ± S.E.M. obtained in three independent experiments. Graphs show quantification of the ratio of REST to β-Actin. *P < 0.05 vs vehicle; **P < 0.05 vs RSV at 12 h. c,d) q RT-PCR and representative Western blot of REST protein incubated for 24 h at 1, 2, 5 and 10 μM of RSV. Bars represent mean ± S.E.M. obtained in four independent experiments. Graphs show quantification of the ratio of REST to β-actin.*P < 0.05 vs vehicle or RSV 1 μM; **P < 0.05 vs all.

cells. SIRT1 knock-down significantly reduced NCX1 and Synapsin-1 mRNA expression as compared to MS SIRT1 (Suppl. Fig. 2c,e), whereas SIRT1 overexpression significantly increased NCX1 and Synapsin-1 mRNA as compared to the empty vector (Suppl. Fig. 2d,f).

SIRT1 does not bind to human REST promoter sequence in vivo

Since RSV regulates gene expression by increasing SIRT1 binding to the promoter sequence (Pezzolla et al., 2015), we investigated whether SIRT1 binds to the REST human promoter (GenBank accession no. AB024498). The rationale for this experiment was that the REST promoter sequence comprises three alternative promoters A, B, and C that regulate the exons a, b and c (Fig. 2o). Interestingly, each exon can splice directly into exon d, which contains the ATG translation initiation site of REST sequence (Koenigsberger et al., 2000; Ravache et al., 2010). Accordingly, we divided the two alternative REST promoter sequences A and B into two different fragments A1, A2 and B1, B2, respectively, whereas the C promoter sequence, termed C1, was left intact (Fig. 2o). ChIP experiments with SIRT1 antibody were performed using specific primers for these five fragments of the REST promoter. In RSV-treated cells, when chromatin was precipitated with SIRT1 antibody, no signal was detected in all REST promoter fragments. However, in SH-SY5Y cells, SIRT1 was able to bind only to the promoter sequence of its known target gene, erythropoietin (EPO) (Dioum et al., 2009), as compared to control IgG (Fig. 2q). This result suggests that SIRT1 does not bind to the REST human promoter sequence in SH-SY5Y cells.

RSV through c-Jun reduces REST mRNA and protein expression

REST human gene promoters have multiple binding sites for the following transcription factors: activator protein-1 (AP-1), nuclear factor-kappa B (NF-kB), and specificity protein 1 (Sp1) (Ravache et al.,

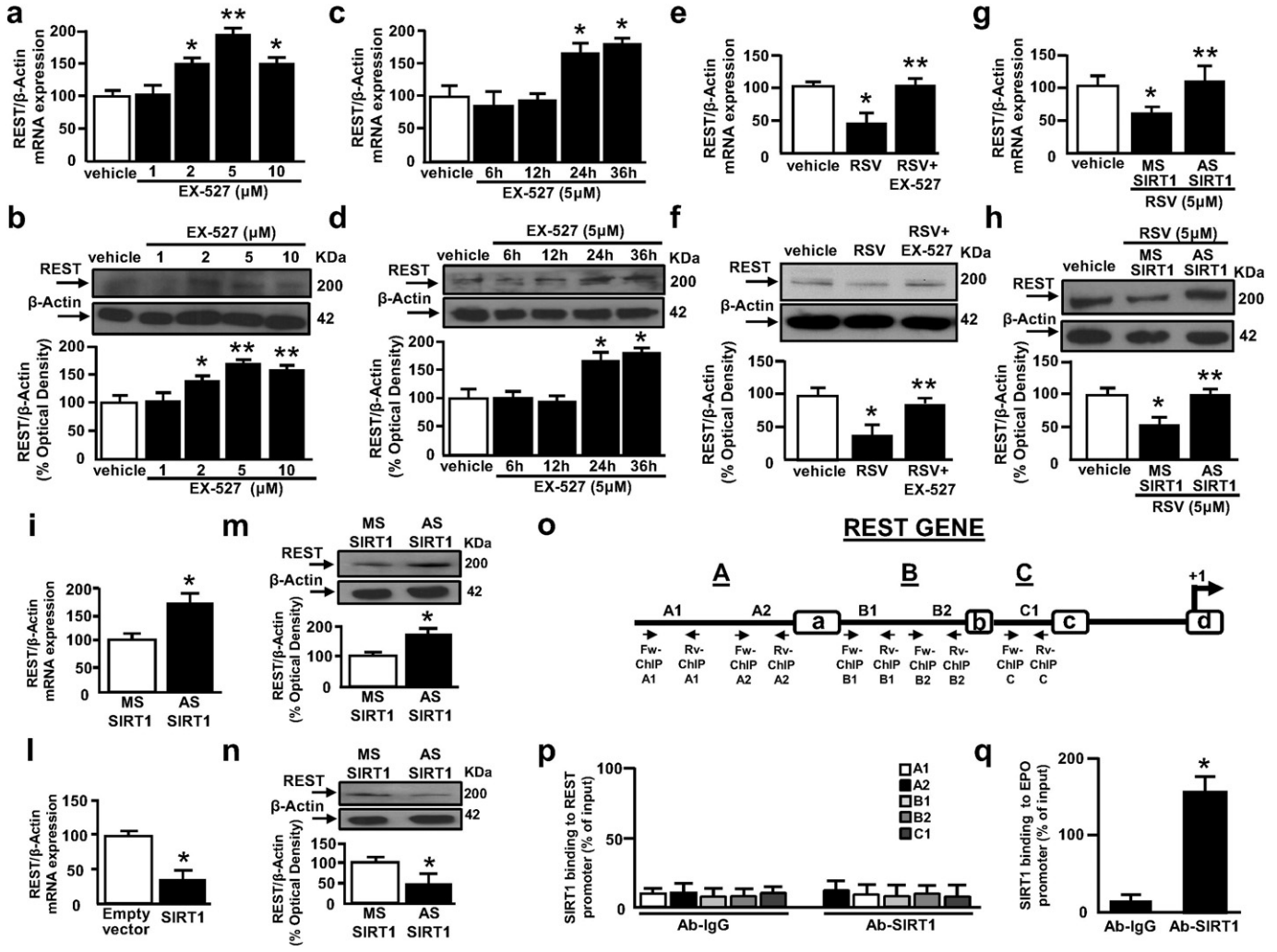

Fig. 2. RSV, *via* SIRT1, decreases REST mRNA and protein without binding to its promoter sequence in SH-SY5Y cells. a–d) q RT-PCR and representative Western blot of REST protein incubated for 24 h at 1, 2, 5 and 10 μM EX-527 (a,b) and for 6, 12, 24 and 36 h at 5 μM EX-527 (c,d). Bars represent mean ± S.E.M. obtained in three independent experiments. Graphs show quantification of the ratio of REST to β-actin. *P < 0.05 vs vehicle**P < 0.05 vs all. e,f) q RT-PCR and representative Western blot of REST mRNA and protein incubated for 24 h with RSV (5 μM) alone or in combination with EX-527 (5 μM). Bars represent mean ± S.E.M. obtained in four independent experiments. *P < 0.05 vs vehicle **P < 0.05 vs RSV alone. g,h) q RT-PCR and representative Western blot of REST mRNA and protein incubated for 24 h with RSV (5 μM) alone or after transfection with AS SIRT1. Bars represent mean ± S.E.M. obtained in three independent experiments. *P < 0.05 vs vehicle **P < 0.05 vs RSV + MS SIRT1. i–n) qRT-PCR (i,l) and representative WB and quantification of REST (m,n) protein expression in SH-SY5Y cells after transfection with MS SIRT1 and AS SIRT1 or pECE (empty vector), and a construct overexpressing SIRT1 (SIRT1). Each column represents the mean ± S.E.M. obtained in four independent experiments (*P < 0.05 vs MS SIRT1 or empty vector). o) Map of the human REST gene indicating the exons a, b, and c downstream of the alternative promoters A, B, and C, respectively, and exon D which contains the translation initiation site, situated as +1, and the PCR primers used to detect the presence of specific DNA sequences in ChIP complexes in A1, A2, B1, B2 and C1 regions of REST promoters. p) ChIP analysis of the A1, A2, B1, B2 and C1 regions of REST promoters performed with anti-SIRT1 and anti-IgG (used as negative control). The binding activity of SIRT1 is graphically represented as the percentage of total input of chromatin DNA. q) ChIP analysis of the EPO promoter region performed with anti-SIRT1 and anti-IgG. The binding activity of SIRT1 is graphically represented as the percentage of total input of chromatin DNA. Bars represent mean ± S.E.M. obtained in three independent experiments. *P < 0.05 *versus* Ab-IgG.

2010). To identify the transcription factors responsible for RSV-induced REST reduction, we treated cells with RSV for 6, 12, and 24 h. Western Blot analysis showed that phospho p65 (p-p65) and p-c-Jun subunits of the NF-kB and AP-1 complexes were increased time dependently at 6, 12 and 24 h (Fig. 3a,b). Interestingly, RSV did not modify Sp1 and Sp3 protein expression (Fig. 3c,d).

Then, to evaluate the role of p65 and c-Jun in RSV-induced REST mRNA and protein reduction, p65 and c-Jun were knocked down in SH-SY5Y cells with antisense oligonucleotides (AS ODNs) (Fig. 3e,f). Notably, AS ODNs for c-Jun (AS c-Jun) and p65 (AS p65) significantly reduced c-Jun and p65 expression by 60% and 70%, respectively, as compared to MS c-Jun and MS p65 (Fig. 3e,f). Interestingly, only AS ODN against c-Jun, but not against p65, reverted the reduction of RSV-induced REST gene and protein expression as compared to vehicle (Fig. 3g,h). Notably, AS c-Jun did not modify REST protein expression in non RSV-treated cells (Suppl. Fig. 3c).

RSV increases c-Jun expression and binding to the AP-1 (b) binding site of REST promoter sequence

qRT-PCR revealed that c-Jun mRNA was significantly increased after 6, 12, and 24 h of RSV (5 μM) treatment, as compared to vehicle (Fig. 4a). Importantly, qRT-PCR and Western blotting at 12 h showed that EX-527 reduced RSV-induced mRNA and protein expression (Fig. 4b,c). Notably, EX-527 did not modify P-c-Jun protein expression in non RSV-treated cells (Suppl. Fig. 3a). Two putative AP-1 binding sites have previously been identified on the REST gene human promoter sequence at −2168/−2162 and −1990/−1984 from the transcription start site (TSS) (+1) (GenBank accession no. AB024498) (Ravache et al., 2010) (Fig. 4d). Thus, to test whether c-Jun could bind directly to these sites, which we named AP-1 (a) (−2168/−2162) and AP-1 (b) (−1990/−1984) (Fig. 4d), after RSV treatment, we performed ChIP. Interestingly, when chromatin from cells treated with vehicle

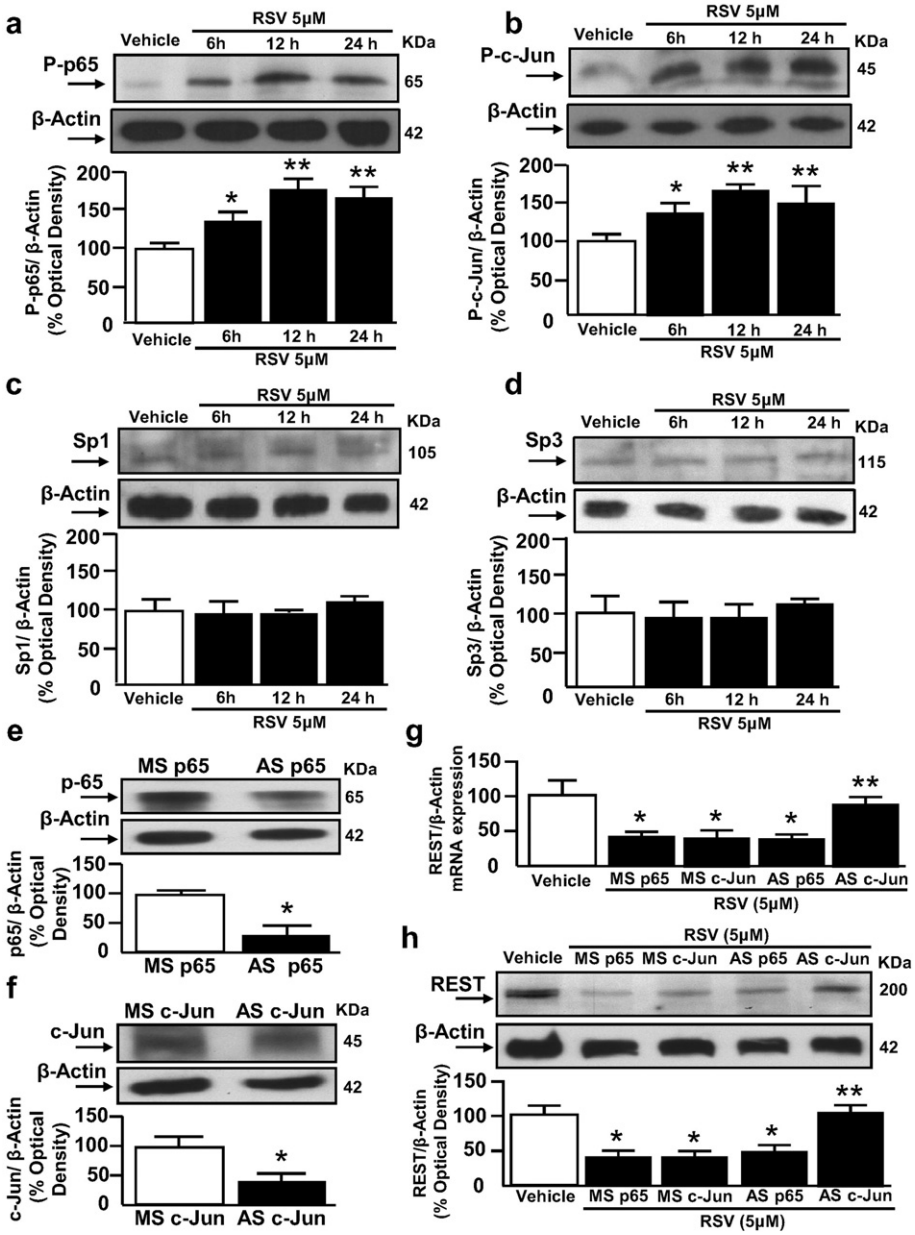

Fig. 3. Effect of RSV on Sp1, Sp3, p65, and c-Jun protein expression and of ODNs against c-Jun and p-65 on RSV-reduced REST mRNA and protein expression in SH-SY5Y cells. a–d) Representative Western blot of P-p65, P-c-Jun, Sp1, and Sp3 proteins at 6, 12, 24 h of RSV (5 μM) exposure. Bars represent mean ± S.E.M. obtained in three independent experiments. Graphs show quantification of the ratio of p65, c-Jun, Sp1, and Sp3 to β-actin. Bars represent mean ± S.E.M. obtained from three independent experiments. P* < 0.05 vs vehicle; **P < 0.05 vs all. e,f) Representative Western blot and quantification of p65 and c-Jun protein expression in SH-SY5Y cells after transfection with missense (MS) p65 and antisense (AS) p65, or MS c-Jun and AS c-Jun. Graphs show quantification of the ratio of p65 or c-Jun to β-actin. Bars represent mean ± S.E.M. obtained from three independent experiments. *P < 0.05 vs MS c-Jun. g,h) qRT-PCR and representative Western blot of the effect of MS and AS for p65 and c-Jun, respectively, on RSV-reduced REST mRNA and protein expression. Bars represent mean ± S.E.M. obtained in four experiments for qRT-PCR and three experiments for Western blot. Graphs show quantification of the ratio of REST to β-actin. Bars represent mean ± S.E.M. obtained from three independent experiments. *P < 0.05 vs vehicle; **P < 0.05 vs MS c-Jun.

was precipitated with the c-Jun antibody, the fragment containing the AP 1 (b) site, but not that including the AP-1 (a) site, was amplified as compared with control IgG. Moreover, the binding activity of c-Jun to AP-1 site (b), but not to AP-1 site (a), was markedly increased after RSV treatment (Fig. 4d,e), in parallel with a decrease in RNA Pol II binding and histone H4 acetylation, as compared to vehicle (Fig. 4f–g). Interestingly, RSV-increased binding activity of c-Jun or the decreased binding of RNA Pol II and histone H4 acetylation to AP-1 (b) site was reverted by co-application of EX-527 (Fig. 4d–g). These data suggest that SIRT1 increases c-Jun binding to the REST gene promoter at the AP 1 (b) site, thereby reducing REST gene transcription.

Resveratrol reduced PCB-95-induced cell death by blocking the increase in REST mRNA and protein levels in SH-SY5Y cells

Exposure of PCB mixture A-1254 for 24 h at 30.6 μM reduces SH-SY5Y cell survival by about 50% through an increase in REST mRNA and protein expression (Formisano et al., 2015a, 2015b). Since the A1254 mixture consists primarily of NDL PCBs (>99%) (Inglefield et al., 2001), we tested the effect of NDL congener PCB-95 on neuronal death. Interestingly, we found that 24 h exposure to PCB-95 (1–16 μM) induced neuronal cell death in a concentration-dependent manner, as evaluated by LDH assay (Fig. 5a). Since 8 μM PCB-95 induced a 50% reduction in cell survival, this concentration was used for further experiments. To investigate

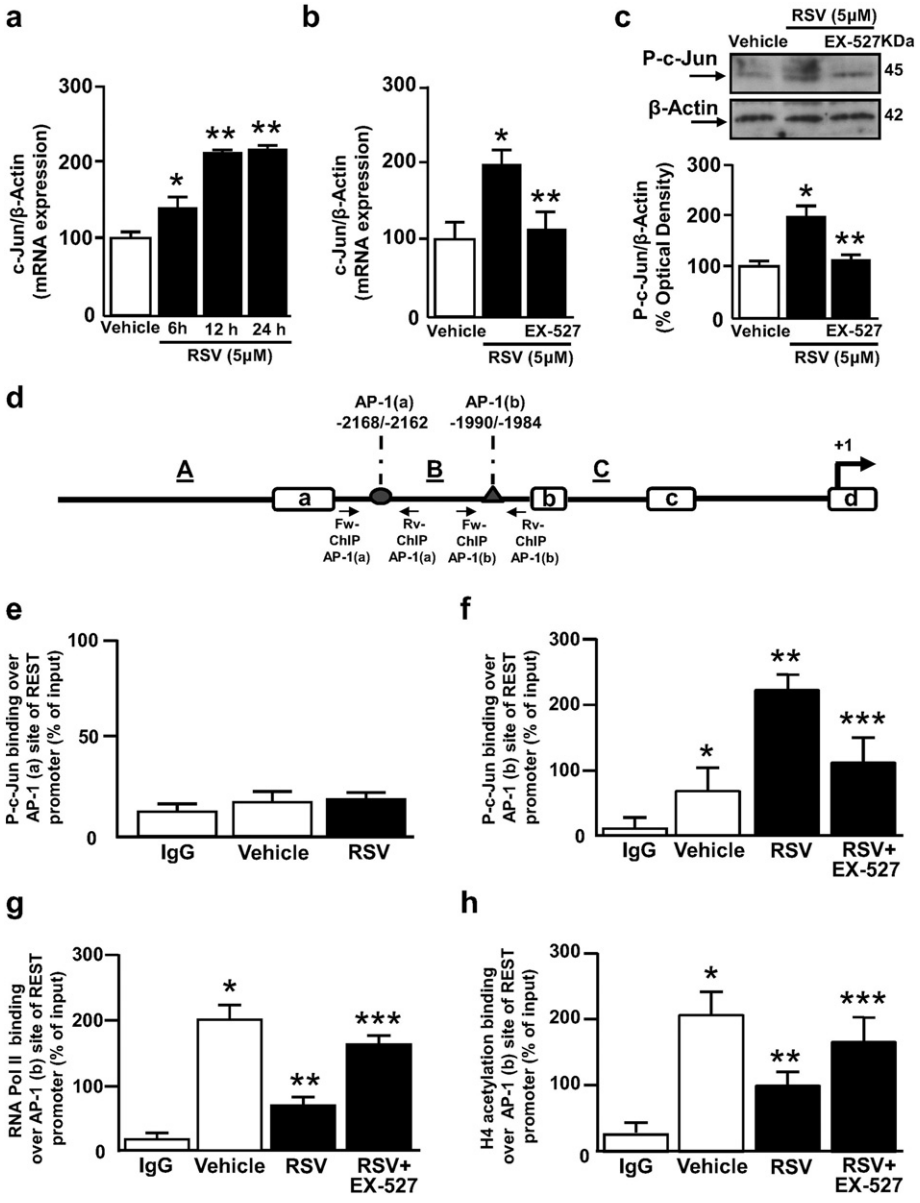

Fig. 4. Effect of EX-527 on RSV-induced c-Jun mRNA and protein expression and on RSV-induced binding to AP-1 (b) site of REST promoter sequence in SH-SY5Y cells. a) qRT-PCR of the effect of RSV on c-Jun mRNA at 6, 12 and 24 h. Bars represent mean ± S.E.M. obtained from four independent experiments. *P < 0.05 vs vehicle **P < 0.05 vs all. b,c) qRT-PCR and representative Western blot of c-Jun mRNA and protein co-incubated for 12 h with RSV (5 μM) alone or in combination with EX-527 (5 μM). Graphs show quantification of the ratio of REST to β-actin. Bars represent mean ± S.E.M. obtained in three independent experiments. *P < 0.05 vs vehicle **P < 0.05 vs RSV alone. d) Schematic representation of human REST gene indicating the exons a, b, and c and the alternative promoters A, B and C; PCR primers used to detect the presence of specific DNA sequences in ChIP complexes in AP-1 (a) and (b) regions of REST promoter. e–h) ChIP of the regions containing the AP-1 (a) and AP-1 (b) sites on the REST gene promoter carried out with anti-c-Jun (e,f) and ChIP of the regions containing the AP-1 (b) site carried out with anti-RNA-POL II and histone H4 acetylation (g,h) in SH-SY5Y cells incubated for 12 h with RSV (5 μM) alone or in combination with EX-527 (5 μM). The binding activity of c-Jun, RNA-POL II, and histone H4 acetylation is graphically represented as the percentage of total input of chromatin DNA. Bars represent mean ± S.E.M. obtained from three independent experiments. *P < 0.05 vs IgG, **P < 0.05 vs vehicle and ***P < 0.05 vs RSV alone.

the role of RSV in PCB-95-induced toxicity, cells were treated with RSV at concentrations of 0.25, 0.5, 1, 5 and 10 μM. LDH assays showed that cell survival significantly improved in a dose dependent manner when cells were co-treated with RSV, as compared to cells exposed to PCB-95 alone (Fig. 5b) and that RSV afforded maximum protection at 5 μM. In addition, at 24 h, PCB-95-induced increase in REST mRNA and protein expression was reverted after RSV (5 μM) treatment (Fig. 5c,d).

Importantly, since REST overexpression diminished H_2O_2-induced cell death reducing production of reactive oxygen species (ROS) and consequent apoptosis activation (Lu et al., 2014) we performed experiments to evaluate whether PCB-95-induced neurotoxicity was associated to oxidative stress and inflammation. In particular, free radical production was monitored by DCF-DA in neuroblastoma cells exposed to PCB 95 (8 μM), RSV (5 μM) alone or in combination. As shown in Supplemental Fig. 4a, after 6 h PCB 95 (8 μM) alone or in combination with RSV (5 μM) failed to modify intracellular ROS levels. On the other hand, ROS levels significantly increased when cells were exposed to H_2O_2, that is a known oxidative stress stimulus (Lu et al., 2014). Furthermore PCB 95 exposure did not cause any change of P-p65 expression (Suppl. Fig. 4b), suggesting a lack of involvement of the inflammation marker in the neurotoxic effect of the pollutant. Collectively these results indicate that oxidative stress and inflammation are not associated to PCB-95-induced neurotoxicity.

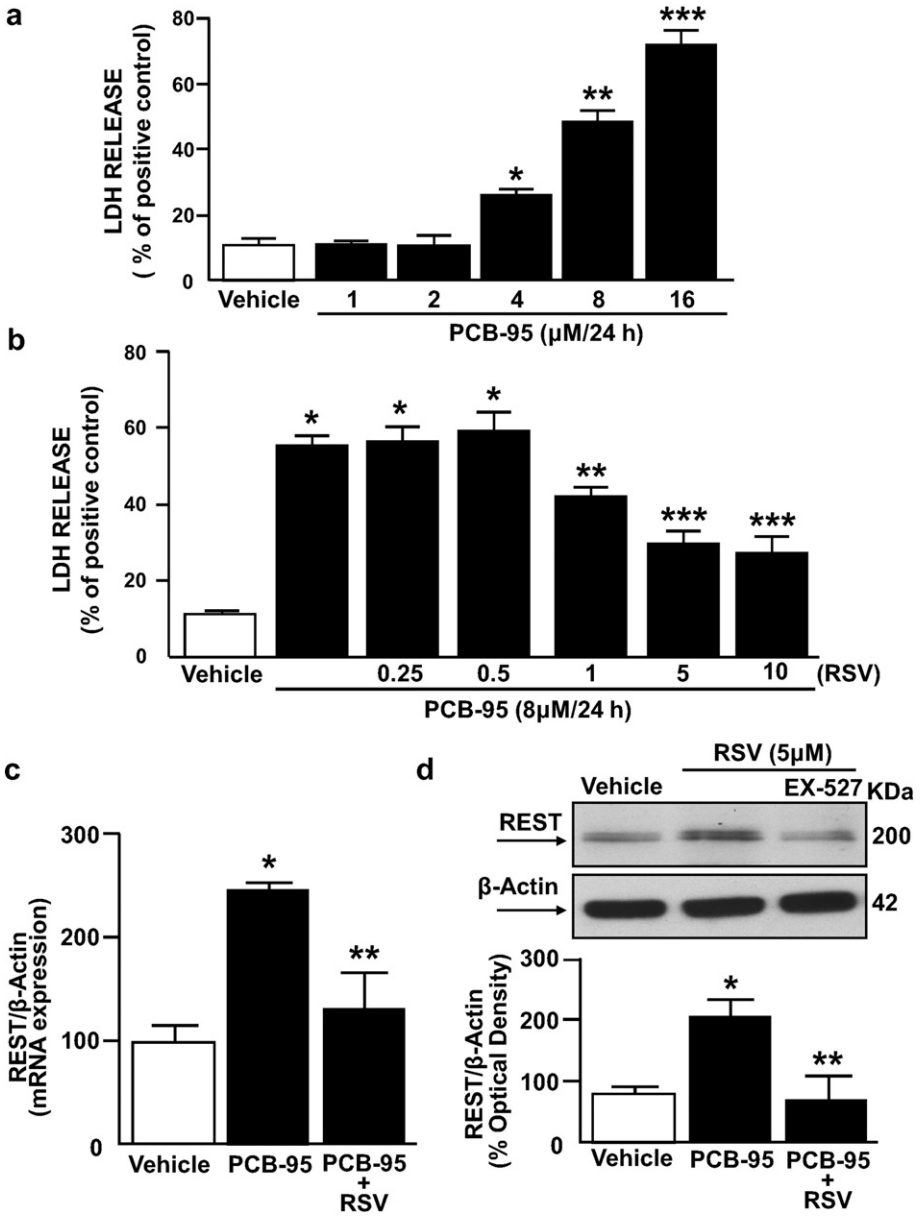

Fig. 5. Effect of PCB-95 alone or in combination with RSV on cell survival and on REST expression in SH-SY5Y cells. a) Effects of 24 h exposure to PCB-95 at 1, 2, 4, 8, and 16 μM on SH-SY5Y cell death, as evaluated by LDH assay. For LDH experiments, 1% Triton X-100 was used as positive control and its value was considered as 100%. Each bar represents mean ± SEM obtained from 5 independent experimental sessions. *P < 0.05 vs vehicle and PCB-95 at 1 and 2 μM, **P < 0.05 vs PCB-95 at 4 μM, ***P < 0.05 vs all. b) Effect of 8 μM PCB-95 at 24 h, alone or with 0.25, 0.5, 1, 5 and 10 μM RSV on LDH release. Bars represent mean ± S.E.M. obtained in four independent experiments. *P < 0.05 vs vehicle; **P < 0.05 vs PCB-95 alone and PCB-95 + RSV at 0.25 and 0.5 μM; ***P < 0.05 vs all. c,d) q RT-PCR and representative Western blot of REST in SH-SY5Y cells treated for 24 h with PCB-95 (8 μM) alone or in combination with RSV (5 μM). Graphs show quantification of the ratio of REST to β-actin. Bars represent mean ± S.E.M. obtained in three independent experiments. *P < 0.05 vs vehicle; **P < 0.05 vs PCB-95 alone.

PCB-95 exposure induced necrotic cell death by activation of SIRT1/c-Jun / REST pathway in cortical neurons

When cortical neurons were exposed to different concentrations of PCB-95 (1–16 μM; Fig. 6a) for 24 h, a dose-related increase in cell death was observed, as evidenced by LDH assay. As in SH-SY5Y cells, PCB-95 at 8 μM was able to reduce cell viability by about 50% and was therefore chosen for our experiments in cortical neurons. It is noteworthy that cell death induced by PCB-95 (8 μM) at 24 h was inhibited in a concentration-related manner when RSV was added to the culture medium at different concentrations (6.25–50 μM) (Fig. 6b); notably, maximum neuroprotection was obtained with 25 μM RSV. Similarly, the increase in REST mRNA and protein expression induced by PCB-95 at 24 h was blocked upon addition of RSV (25 μM) (Fig. 6c,d). Notably, PCB-95-induced increase in calpain expression was blocked by RSV co-application; in contrast, the apoptotic marker procaspase-3 was unmodified (Fig. 6e,f). Moreover, PCB-95-induced decrease in P-c-Jun was reverted by RSV, as compared to the vehicle (Fig. 6g).

We next investigated the function of c-Jun and SIRT1 in RSV-blocked PCB-95-induced REST gene and gene product increase. To this aim, we knocked down c-Jun and SIRT1 with ODN for c-Jun (AS c-Jun) and with siRNA for SIRT1 (siSIRT1). Notably, siSIRT1 and AS ODNs for c-Jun significantly reduced SIRT1 and c-Jun expression by 55% and 65%, respectively (Suppl. Fig. 3b,d).

Intriguingly, transfection of AS c-Jun and siSIRT1 blocked RSV capability to reduce PCB-95-induced REST mRNA and protein expression as

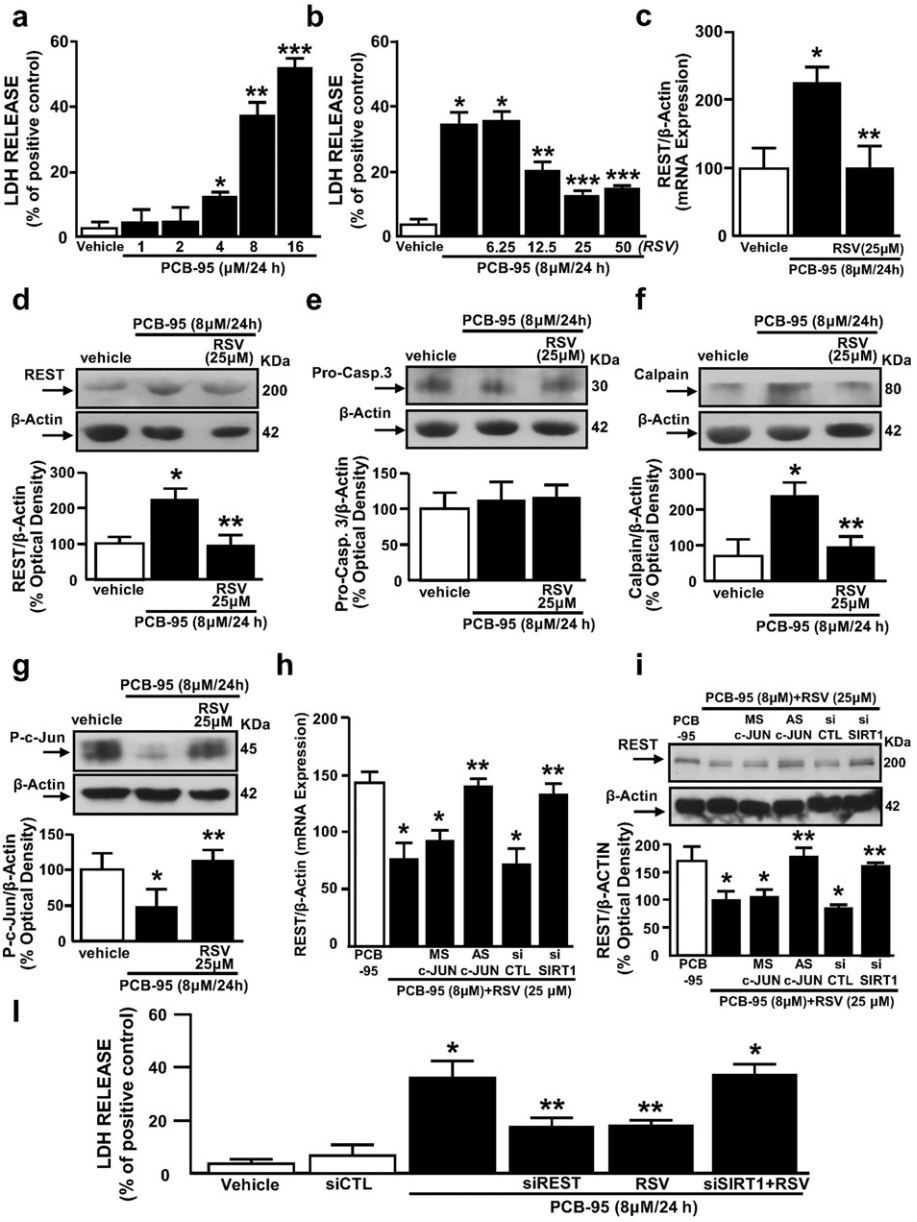

Fig. 6. Effect of PCB-95 alone or in combination with RSV on neuronal survival and on P-c-Jun, SIRT1, and REST expression. a) Effects of 24 h exposure to PCB-95 at 1, 2, 4, 8, and 16 μM on cortical neurons death, measured by LDH. Each bar represents mean ± SEM obtained from four independent experimental sessions.*P < 0.05 vs vehicle, PCB-95 at 1 and 2 μM;**P < 0.05 vs PCB-95 at 4 μM and ***P < 0.05 vs all. b) Effect of 8 μM PCB-95 at 24 h, alone or with 6.25, 12.5, 25, and 50 μM RSV on LDH release. Bars represent mean ± S.E.M. obtained in five independent experiments. *P < 0.05 vs vehicle; **P < 0.05 vs vehicle, PCB-95 alone and PCB-95 + RSV 6.25 μM; ***P < 0.05 vs all. c) qRT-PCR of REST mRNA in neurons treated for 24 h with PCB-95 (8 μM) alone or in combination with RSV (25 μM). Bars represent mean ± S.E.M. obtained in three independent experiments. *P < 0.05 vs vehicle and **P < 0.05 vs PCB-95 alone. d–g) Western blots of REST, pro-caspase 3, calpain, and P-c-Jun protein levels in vehicle after 24 h of PCB-95 (8 μM), alone or in combination with RSV (25 μM). Graphs show quantification of the ratio of REST, pro-caspase 3, calpain and c-Jun to β-actin. Bars represent mean ± S.E.M. obtained from three independent experiments. *P < 0.05 vs vehicle; **P < 0.05 vs PCB-95 alone. h,i) qRT-PCR and Western blot analysis of REST in neurons transfected with MS and AS ODNs for c-Jun or of siRNAs, siCTL, and siSIRT1 for SIRT1 to block the reducing effect of RSV on PCB-95-induced REST gene and gene product expression. Bars represent mean ± S.E.M. obtained in four independent experiments. Graphs show quantification of the ratio of REST to β-actin. *P < 0.05 vs PCB-95 alone; **P < 0.05 vs PCB-95 + RSV. l) Effects of 24 h exposure to PCB-95 8 μM on cortical neuronal death, as measured by LDH in vehicle, siCTL and when PCB-95 was administered alone or after siREST transfection and when PCB-95 was administered in combination with RSV alone or after siSIRT1 transfection. For LDH experiments, 1% Triton X-100 was used as positive control and its value was considered as 100%. Each bar represents the mean ± S.E.M. obtained from five independent experiments. *P < 0.05 *versus* vehicle or siCTL, ** P < 0.05 *versus* PCB-95 alone.

compared to RSV-treated cells and transfected with MS c-Jun and siCTL, respectively (Fig. 6h,i). Then, to evaluate the role of REST in PCB-95-induced toxicity, we knocked down its expression. Particularly, siRNA for REST was recently published (Formisano et al., 2013, 2015b). Unsurprisingly, siREST transfection reduced PCB-95-induced neurotoxicity (Fig. 6l). Interestingly, co-incubation with RSV significantly reduced the detrimental effect of PCB-95, as compared to vehicle (Fig. 6l). Notably, siRNA transfection against SIRT1 completely abolished RSV-induced neuroprotection in cortical neurons exposed to PCB-95 (Fig. 6l).

Discussion

In the present study, we showed that resveratrol (RSV) reduces REST expression at the transcriptional level *via* activation of SIRT1. As a result,

SIRT1 increases c-Jun mRNA and protein expression, thus causing an increase in its binding activity to the REST human gene promoter sequence in SH-SY5Y cells. In particular, overexpression of SIRT1 suppressed REST expression, whereas the specific SIRT1 inhibitor EX-527 (Yan et al., 2013) increased it. In addition, we showed that in cortical neurons RSV, through SIRT1 and c-Jun, suppressed PCB-95-induced neurotoxicity caused by REST mRNA and protein upregulation. To our knowledge, this is the first report showing that RSV downregulates REST in neuronal cells. Furthermore, RSV-induced suppression of REST was reversed by EX-527, a well known inhibitor of SIRT1, thereby suggesting that RSV suppressed REST expression through SIRT1 activation at the transcriptional level. Indeed, we identified c-Jun, a subunit of the AP-1 complex, as the transcriptional factor that down-regulates REST after RSV treatment. More specifically, we evidenced that of the four identified putative transcription factors regulating REST (Ravache et al., 2010), RSV was able to increase the phosphorylation of only c-Jun and p65 proteins, whereas Sp1, Sp3, which are known to regulate REST mRNA expression (Ravache et al., 2010; Formisano et al., 2015a), were unmodified. Most important, c-Jun, but not p65, knockdown was able to block RSV-induced REST mRNA and protein expression in SH-SY5Y neuroblastoma cells.

Such evidence led us to a second major finding. Indeed, to the best of our knowledge, this is the first report showing that c-Jun is a REST transcriptional repressor. This result expands findings from previous reports showing that Jun homodimers may be activators or repressors depending on the context of the promoter, the sequence of the cognate DNA-binding site, the cell phenotype, and the environmental milieu of the cell, *i.e.*, conditions that favor quiescence or proliferation (Ubeda et al., 1999). Moreover, within the human REST gene promoter, we identified two AP-1 motifs (AP-1 a and AP-1 b), located at −2168/−2162 and −1990/−1984 from the transcription start site (TSS), as possible molecular determinants involved in c-Jun-induced REST regulation (Ravache et al., 2010). Notably, ChIP revealed that RSV induced c-Jun binding exclusively to the AP-1 (b) site, which was completely abolished when cells were treated with the SIRT 1 inhibitor EX-527 a result suggesting the involvement of SIRT 1 in c-Jun-induced REST regulation. On the other hand, we found that in RSV-treated cells, SIRT1 did not bind to any of the REST promoter fragments. Given these results, we speculate that REST downregulation induced by RSV and mediated by SIRT1 is not due to the direct binding of SIRT1 to the REST gene promoter but, rather, to the participation of c-Jun. Moreover, evidence for the interplay between c-Jun and SIRT1 is that the increase in RSV-induced c-Jun mRNA and protein expression was reverted by EX-527 treatment. Our results also characterized the binding site of c-Jun on REST human promoter; in fact, only the AP-1 (b) site of the two putative AP-1 elements present on the REST promoter sequence was important for c-Jun binding after RSV treatment. Interestingly, c-Jun binding to the AP-1 (b) site was reverted by EX-527, thus confirming even further the key role played by SIRT1 in this interaction.

Our results are in accordance with previous reports demonstrating that RSV causes an increase in c-Jun mRNA (Shih et al., 2002). Considering the key role played by SIRT1 in this process, we could hypothesize that RSV was able to increase SIRT1 binding to c-Jun gene promoter sequence. Such increased SIRT1 binding then determined an increase in its mRNA and protein expression that, in turn, by interacting with REST promoter sequence, downregulated its expression.

Evidence for RSV neuroprotective effect also emerged when cells were treated with non-dioxin like (NDL) polychlorinated biphenyl 95 (PCB-95). We found that NDL-PCB-95 induced neuronal cell death in a concentration dependent manner and that RSV reverted this effect. Interestingly, exposure to NDL-PCB-95 at 8 μM damaged approximately 50% of SH-SY5Y cells and cortical neurons. However, RSV counteracted PCB-induced cell death at 5 μM in SH-SY5Y and at 25 μM in cortical neurons. These results confirm earlier findings demonstrating that RSV induces neuroprotection at 25 μM in neuronal primary cultures (Sakata et al., 2010) and at 5 μM in SH-SY5Y cells (Lee et al., 2007), and that primary neurons are more resistant to RSV neuroprotection.

Intriguingly, we found that SIRT1 knockdown blocked RSV- induced neuroprotection in neurons, thereby corroborating the hypothesis that RSV *via* SIRT1 activation determines neuronal survival. In fact, specific siRNAs against SIRT1 are known to abolish RSV-induced neuroprotection in *in vitro* models of brain ischemia (Wang et al., 2013) and in retinal ganglion cells after H_2O_2 treatment (Khan et al., 2012).

Moreover our results are also in line with the neuroprotective role played by c-Jun. In fact, c-Jun over-expressing cells are more resistant to okadaic acid-induced apoptosis (Dragunow et al., 2000) and its induction in ischemic conditioning is able to rescue CA1 hippocampal from neuronal death (Sommer et al., 1995).

It has been shown that REST protects against oxidative stress down-regulating apoptotic gene expression whereas in this paper we found that REST up-regulation induced by PCB-95 determines cell-death. However, the toxic pathways triggered by oxidative stress and PCB-95 seem to be different. In fact oxidative stress, inflammation and apoptosis do not occur in our experimental conditions. Indeed PCB-95 exposure failed to increase ROS production and the expression of P-p65 protein, a marker of inflammation. Furthermore in PCB-95 treated cells a necrotic and not an apoptotic cell death occur. Our findings suggest that oxidative stress, apoptosis and inflammation are not associated to PCB-95 induced neurotoxicity in our experimental model, and that RSV-induced neuroprotection is mediated by SIRT1/c-Jun pathway, that counteracts REST increase. Consistently, we have previously shown that PCB mixture A1254 through REST induces necrotic cell death in neurons (Formisano et al., 2011, 2015a, 2015b). Regarding the PCB concentrations tested in the present study, they have already been used in previous reports and are within the range of PCBs detected in wildlife animals (Mariussen et al., 2002). Specifically, PCB-95, but not other PCBs or polybrominated diphenyl ethers (PBDEs), is significantly higher in post-mortem brains of children with a syndromic form of autism, compared with neurotypical controls (Mitchell et al., 2012). Furthermore, PCB-95 crosses the blood–brain barrier and can interact with targets (Kania-Korwel et al., 2012).

Collectively, these results indicate that resveratrol through SIRT1/c-Jun pathway regulates REST expression at the basal level in SH-SY5Y neuronal cells and is involved in the neurotoxic effect of NDL PCB-95. Furthermore, these results indicate that resveratrol exerts a neuroprotective effect against the toxic effect of PCBs by increasing SIRT1 activity that in turn causes a reduction in c-Jun binding to the REST promoter sequence.

Supplementary data to this article can be found online at http://dx.doi.org/10.1016/j.taap.2015.08.010.

Conflict of interest statement

The authors declare that there is no conflict of interest.

Authorship contributions

Conceived and designed the experiments: NG, GL, SA, AS, GDR and LF. Performed the experiments: NG, GL, PM, GDR, and LF. Analyzed the data: NG, GL, AS, GDR, and LF. Contributed reagents/materials/analysis tools NG, GL, GDR, LMT and LF:. Wrote the paper: LMTC GDR and LF

Transparency document

The Transparency document associated with this article can be found, in online version.

Acknowledgments

We thank, Mr. Carmine Capitale for technical support and Dr Paola Merolla for editorial revision.

This work was supported by grants: from [COFIN2008], Ricerca finalizzata [2009] PON 01_01602 and PON 03PE_00146_1.

References

Amoroso, S., Gioielli, A., Cataldi, M., Di Renzo, G., Annunziato, L., 1999. In the neuronal cell line SH-SY5Y, oxidative stress-induced free radical overproduction causes cell death without any participation of intracellular Ca^{2+} increase. Biochim. Biophys. Acta Mol. Cell Res. 1452, 151–160.

Brunet, A., Sweeney, L.B., Sturgill, J.F., Chua, K.F., Greer, P.L., Lin, Y., Tran, H., Ross, S.E., Mostoslavsky, R., Cohen, H.Y., Hu, L.S., Cheng, H.L., Jedrychowski, M.P., Gygi, S.P., Sinclair, D.A., Alt, F.W., Greenberg, M.E., 2004. Stress-dependent regulation of FOXO transcription factors by the SIRT1 deacetylase. Science 303, 2011–2015.

Busch, F., Mobasheri, A., Shayan, P., Stahlmann, R., Shakibaei, M., 2012. Sirt-1 is required for the inhibition of apoptosis and inflammatory responses in human tenocytes. J. Biol. Chem. 287, 25770–25781.

Cocco, S., Secondo, A., Del Viscovo, A., Procaccini, C., Formisano, L., Franco, C., Esposito, A., Scorziello, A., Matarese, G., Di Renzo, G., Canzoniero, L.M., 2015. Polychlorinated biphenyls induce mitochondrial dysfunction in SH-SY5Y neuroblastoma cells. PLoS One 10, e0129481.

Dioum, E.M., Chen, R., Alexander, M.S., Zhang, Q., Hogg, R.T., Gerard, R.D., Garcia, J.A., 2009. Regulation of hypoxia-inducible factor 2alpha signaling by the stress-responsive deacetylase sirtuin 1. Science 324, 1289–1293.

Donmez, G., 2012. The neurobiology of sirtuins and their role in neurodegeneration. Trends Pharmacol. Sci. 33, 494–501.

Donmez, G., Outeiro, T.F., 2013. SIRT1 and SIRT2: emerging targets in neurodegeneration. EMBO Mol. Med. 5, 344–352.

Dragunow, M., Xu, R., Walton, M., Woodgate, A., Lawlor, P., MacGibbon, G.A., Young, D., Gibbons, H., Lipski, J., Muravlev, A., Pearson, A., During, M., 2000. c-Jun promotes neurite outgrowth and survival in PC12 cells. Brain Res. Mol. Brain Res. 83, 20–33.

Formisano, L., Noh, K., Miyawaki, T., Mashiko, T., Bennett, M., Zukin, R., 2007. Ischemic insults promote epigenetic reprogramming of mu opioid receptor expression in hippocampal neurons. Proc. Natl. Acad. Sci. U. S. A. 104, 4170–4175.

Formisano, L., Guida, N., Cocco, S., Secondo, A., Sirabella, R., Ulianich, L., Paturzo, F., Di Renzo, G., Canzoniero, L.M., 2011. The repressor element 1-silencing transcription factor is a novel molecular target for the neurotoxic effect of the polychlorinated biphenyl mixture aroclor 1254 in neuroblastoma SH-SY5Y cells. J. Pharmacol. Exp. Ther. 338, 997–1003.

Formisano, L., Guida, N., Valsecchi, V., Pignataro, G., Vinciguerra, A., Pannaccione, A., Secondo, A., Boscia, F., Molinaro, P., Sisalli, M.J., Sirabella, R., Casamassa, A., Canzoniero, L.M., Di Renzo, G., Annunziato, L., 2013. NCX1 is a new rest target gene: role in cerebral ischemia. Neurobiol. Dis. 50, 76–85.

Formisano, L., Guida, N., Laudati, G., Boscia, F., Esposito, A., Secondo, A., Di Renzo, G., Canzoniero, L.M., 2015a. Extracellular signal-related kinase 2/specificity protein 1/specificity protein 3/repressor element-1 silencing transcription factor pathway is involved in Aroclor 1254-induced toxicity in SH-SY5Y neuronal cells. J. Neurosci. Res. 93 (1), 167–177.

Formisano, L., Guida, N., Laudati, G., Mascolo, L., Di Renzo, G., Canzoniero, L.M., 2015b. MS-275 inhibits aroclor 1254-induced SH-SY5Y neuronal cell toxicity by preventing the formation of the HDAC3/REST complex on the synapsin-1 promoter. J. Pharmacol. Exp. Ther. 352, 236–243.

Formisano, L., Guida, N., Valsecchi, V., Cantile, M., Cuomo, O., Vinciguerra, A., Laudati, G., Pignataro, G., Sirabella, R., Di Renzo, G., Annunziato, L., 2015c. Sp3/REST/HDAC1/HDAC2 complex represses and Sp1/HIF-1/p300 complex activates ncx1 gene transcription, in brain ischemia and in ischemic brain preconditioning, by epigenetic mechanism. J. Neurosci. 35, 7332–7348.

Giesy, J.P., Kannan, K., 1998. Dioxin-like and non-dioxin-like toxic effects of polychlorinated biphenyls (PCBs): implications for risk assessment. Crit. Rev. Toxicol. 28, 511–569.

Guida, N., Laudati, G., Galgani, M., Santopaolo, M., Montuori, P., Triassi, M., Di Renzo, G., Canzoniero, L.M., Formisano, L., 2014. Histone deacetylase 4 promotes ubiquitin-dependent proteasomal degradation of Sp3 in SH-SY5Y cells treated with di(2-ethylhexyl)phthalate (DEHP), determining neuronal death. Toxicol. Appl. Pharmacol. 280 (1), 190–198.

Hsieh, Y.S., Yang, S.F., Chu, S.C., Kuo, D.Y., 2008. Interrupting activator protein-1 signaling in conscious rats can modify neuropeptide Y gene expression and feeding behavior of phenylpropanolamine. J. Neurochem. 104, 50–61.

Iannotti, F.A., Barrese, V., Formisano, L., Miceli, F., Taglialatela, M., 2013. Specification of skeletal muscle differentiation by repressor element-1 silencing transcription factor (REST)-regulated Kv7.4 potassium channels. Mol. Biol. Cell 24, 274–284.

Inglefield, J.R., Mundy, W.R., Shafer, T.J., 2001. Inositol 1,4,5-triphosphate receptor-sensitive Ca(2+) release, store-operated Ca(2+) entry, and cAMP responsive element binding protein phosphorylation in developing cortical cells following exposure to polychlorinated biphenyls. J. Pharmacol. Exp. Ther. 297, 762–773.

Kaneko, N., Hwang, J.Y., Gertner, M., Pontarelli, F., Zukin, R.S., 2014. Casein kinase 1 suppresses activation of REST in insulted hippocampal neurons and halts ischemia-induced neuronal death. J. Neurosci. 34, 6030–6039.

Kania-Korwel, I., Barnhart, C.D., Stamou, M., Truong, K.M., El-Komy, M.H., Lein, P.J., Veng-Pedersen, P., Lehmler, H.J., 2012. 2,2′,3,5′,6-Pentachlorobiphenyl (PCB 95) and its hydroxylated metabolites are enantiomerically enriched in female mice. Environ. Sci. Technol. 46, 11393–11401.

Khan, R.S., Fonseca-Kelly, Z., Callinan, C., Zuo, L., Sachdeva, M.M., Shindler, K.S., 2012. SIRT1 activating compounds reduce oxidative stress and prevent cell death in neuronal cells. Front. Cell. Neurosci. 6, 63.

Koenigsberger, C., Chicca, J.J., Amoureux, M.C., Edelman, G.M., Jones, F.S., 2000. Differential regulation by multiple promoters of the gene encoding the neuron-restrictive silencer factor. Proc. Natl. Acad. Sci. U. S. A. 97, 2291–2296.

Lee, M.K., Kang, S.J., Poncz, M., Song, K.J., Park, K.S., 2007. Resveratrol protects SH-SY5Y neuroblastoma cells from apoptosis induced by dopamine. Exp. Mol. Med. 39, 376–384.

Li, F., Gong, Q., Dong, H., Shi, J., 2012. Resveratrol, a neuroprotective supplement for Alzheimer's disease. Curr. Pharm. Des. 18, 27–33.

Lu, T., Aron, L., Zullo, J., Pan, Y., Kim, H., Chen, Y., Yang, T.-H., Kim, H.-M., Drake, D., Liu, X.S., Bennett, D.A., Colaiacovo, M.P., Yankner, B.A., 2014. REST and stress resistance in ageing and Alzheimer's disease. Nature 507, 448–454.

Mancuso, R., del Valle, J., Modol, L., Martinez, A., Granado-Serrano, A.B., Ramirez-Núñez, O., Pallás, M., Portero-Otin, M., Osta, R., Navarro, X., 2014. Resveratrol improves motoneuron function and extends survival in SOD1(G93A) ALS mice. Neurotherapeutics 11, 419–432.

Mariussen, E., Myhre, O., Reistad, T., Fonnum, F., 2002. The polychlorinated biphenyl mixture aroclor 1254 induces death of rat cerebellar granule cells: the involvement of the N-methyl-D-aspartate receptor and reactive oxygen species. Toxicol. Appl. Pharmacol. 179, 137–144.

McFarland, V.A., Clarke, J.U., 1989. Environmental occurrence, abundance, and potential toxicity of polychlorinated biphenyl congeners: considerations for a congener-specific analysis. Environ. Health Perspect. 81, 225–239.

Mitchell, M.M., Woods, R., Chi, L.H., Schmidt, R.J., Pessah, I.N., Kostyniak, P.J., LaSalle, J.M., 2012. Levels of select PCB and PBDE congeners in human postmortem brain reveal possible environmental involvement in 15q11–q13 duplication autism spectrum disorder. Environ. Mol. Mutagen. 53, 589–598.

Morris, K.C., Lin, H.W., Thompson, J.W., Perez-Pinzon, M.A., 2011. Pathways for ischemic cytoprotection: role of sirtuins in caloric restriction, resveratrol, and ischemic preconditioning. J. Cereb. Blood Flow Metab. 31, 1003–1019.

Noh, K.M., Hwang, J.Y., Follenzi, A., Athanasiadou, R., Miyawaki, T., Greally, J.M., Bennett, M.V., Zukin, R.S., 2012. Repressor element-1 silencing transcription factor (REST)-dependent epigenetic remodeling is critical to ischemia-induced neuronal death. Proc. Natl. Acad. Sci. U. S. A. 109, E962–E971.

Ohkawa, T., Ueki, N., Taguchi, T., Shindo, Y., Adachi, M., Amuro, Y., Hada, T., Higashino, K., 1999. Stimulation of hyaluronan synthesis by tumor necrosis factor-alpha is mediated by the p50/p65 NF-kappa B complex in MRC-5 myofibroblasts. Biochim. Biophys. Acta 1448, 416–424.

Pannaccione, A., Secondo, A., Scorziello, A., Cali, G., Taglialatela, M., Annunziato, L., 2005. Nuclear factor-kappaB activation by reactive oxygen species mediates voltage-gated K+ current enhancement by neurotoxic beta-amyloid peptides in nerve growth factor-differentiated PC-12 cells and hippocampal neurones. J. Neurochem. 94, 572–586.

Peterson, T.C., Peterson, M.R., Robertson, H.A., During, M., Dragunow, M., 2002. Selective down-regulation of c-jun gene expression by pentoxifylline and c-jun antisense interrupts platelet-derived growth factor signaling: pentoxifylline inhibits phosphorylation of c-Jun on serine 73. Mol. Pharmacol. 61, 1476–1488.

Pezzolla, D., López-Beas, J., Lachaud, C.C., Domínguez-Rodríguez, A., Smani, T., Hmadcha, A., Soria, B., 2015. Resveratrol ameliorates the maturation process of β-cell-like cells obtained from an optimized differentiation protocol of human embryonic stem cells. PLoS One 10, e0119904.

Rahman, S., Islam, R., 2011. Mammalian Sirt1: insights on its biological functions. Cell Commun. Signal. 9, 11.

Ravache, M., Weber, C., Mérienne, K., Trottier, Y., 2010. Transcriptional activation of REST by Sp1 in Huntington's disease models. PLoS One 5, e14311.

Rodenas-Ruano, A., Chávez, A.E., Cossio, M.J., Castillo, P.E., Zukin, R.S., 2012. REST-dependent epigenetic remodeling promotes the developmental switch in synaptic NMDA receptors. Nat. Neurosci. 15, 1382–1390.

Sakata, Y., Zhuang, H., Kwansa, H., Koehler, R.C., Doré, S., 2010. Resveratrol protects against experimental stroke: putative neuroprotective role of heme oxygenase 1. Exp. Neurol. 224, 325–329.

Seo, J.S., Moon, M.H., Jeong, J.K., Seol, J.W., Lee, Y.J., Park, B.H., Park, S.Y., 2012. SIRT1, a histone deacetylase, regulates prion protein-induced neuronal cell death. Neurobiol. Aging 33, 1110–1120.

Shih, A., Davis, F.B., Lin, H.Y., Davis, P.J., 2002. Resveratrol induces apoptosis in thyroid cancer cell lines via a MAPK- and p53-dependent mechanism. J. Clin. Endocrinol. Metab. 87, 1223–1232.

Sirabella, R., Secondo, A., Pannaccione, A., Molinaro, P., Formisano, L., Guida, N., Di Renzo, G., Annunziato, L., Cataldi, M., 2012. ERK1/2, p38, and JNK regulate the expression and the activity of the three isoforms of the Na(+) /Ca(2+) exchanger, NCX1, NCX2, and NCX3, in neuronal PC12 cells. J. Neurochem. 122 (5), 911–922.

Sommer, C., Gass, P., Kiessling, M., 1995. Selective c-JUN expression in CA1 neurons of the gerbil hippocampus during and after acquisition of an ischemia-tolerant state. Brain Pathol. 5, 135–144.

Tang, B.L., 2010. Resveratrol is neuroprotective because it is not a direct activator of Sirt1-A hypothesis. Brain Res. Bull. 81, 359–361.

Ubeda, M., Vallejo, M., Habener, J.F., 1999. CHOP enhancement of gene transcription by interactions with Jun/Fos AP-1 complex proteins. Mol. Cell. Biol. 19, 7589–7599.

Vinciguerra, A., Formisano, L., Cerullo, P., Guida, N., Cuomo, O., Esposito, A., Di Renzo, G., Annunziato, L., Pignataro, G., 2014. MicroRNA-103-1 selectively downregulates brain NCX1 and its inhibition by anti-miRNA ameliorates stroke damage and neurological deficits. Mol. Ther. 22 (10), 1829–1838.

Wang, L.M., Wang, Y.J., Cui, M., Luo, W.J., Wang, X.J., Barber, P.A., Chen, Z.Y., 2013. A dietary polyphenol resveratrol acts to provide neuroprotection in recurrent stroke models by regulating AMPK and SIRT1 signaling, thereby reducing energy requirements during ischemia. Eur. J. Neurosci. 37, 1669–1681.

Weintraub, M., Birnbaum, L., 2008. Catfish consumption as a contributor to elevated PCB levels in a non-Hispanic black subpopulation. Environ. Res. 107, 412–417.

Wu, Y., Li, X., Zhu, J.X., Xie, W., Le, W., Fan, Z., Jankovic, J., Pan, T., 2011. Resveratrol-activated AMPK/SIRT1/autophagy in cellular models of Parkinson's disease. Neurosignals 19, 163–174.

Yan, W., Fang, Z., Yang, Q., Dong, H., Lu, Y., Lei, C., Xiong, L., 2013. SirT1 mediates hyperbaric oxygen preconditioning-induced ischemic tolerance in rat brain. J. Cereb. Blood Flow Metab. 33, 396–406.